

High-latitude dust clouds LDN 183 and LDN 169: distances and extinctions*

V. Straižys¹, R. P. Boyle², J. Zdanavičius¹, R. Janusz³, C. J. Corbally², U. Munari⁴, B.-G. Andersson⁵, K. Zdanavičius¹, A. Kazlauskas¹, M. Maskoliūnas¹, K. Černis¹, and M. Macijauskas¹

Received 8 August 2017 / Accepted 11 December 2017

ABSTRACT

Interstellar extinction is investigated in a $2^{\circ} \times 2^{\circ}$ area containing the dust and molecular clouds LDN 183 (MBM 37) and LDN 169, which are located at RA = $15^{\rm h}$ $54^{\rm m}$, Dec = -3° . The study is based on a photometric classification in spectral and luminosity classes of 782 stars selected from the catalogs of 1299 stars down to V = 20 mag observed in the Vilnius seven-color system. For control, the MK types for the 18 brightest stars with V between 8.5 and 12.8 mag were determined spectroscopically. For 14 stars, located closer than 200 pc, distances were calculated from trigonometric parallaxes taken from the *Gaia* Data Release 1. For about 70% of the observed stars, two-dimensional spectral types, interstellar extinctions A_V , and distances were determined. Using 57 stars closer than 200 pc, we estimate that the front edge of the clouds begins at 105 ± 8 pc. The extinction layer in the vicinities of the clouds can be about 20 pc thick. In the outer parts of the clouds and between the clouds, the extinction is 0.5–2.0 mag. Behind the Serpens/Libra clouds, the extinction range does not increase; this means that the dust layer at 105 pc is a single extinction source.

Key words. stars: fundamental parameters – ISM: clouds – dust, extinction – ISM: individual objects: LDN 169 – ISM: individual objects: LDN 183 (MBM 37)

1. Introduction

Mapping distances and the geometry of local interstellar clouds is an important tool for understanding the evolution of interstellar matter in the solar vicinity. The data on their density and the extinction properties, together with polarization and dust emission, provide critical constraints on the dust grain sizes and composition.

The dust cloud LDN 183 (Lynds 1962) and the related molecular cloud MBM 37 (Magnani et al. 1985) are part of the high-latitude complex of interconnected dust and molecular clouds that also includes the clouds LDN 169, LDN 134 (MBM 36), LDN 1780 (MBM 33), and MBM 38, which are located at the border between the Serpens Caput and Libra constellations at the galactic latitude $b \sim +37^{\circ}$. It is thought that these clouds are related to the surface of Loop I of the Local Bubble (Franco 1989a; Lallement et al. 2003). The cloud LDN 183 and the nearby LDN 134 belong to a group of starless clouds with very dense and low-temperature cores with prestellar condensations and the coreshine phenomenon (Pagani et al. 2003, 2004; Steinacker et al. 2010; Juvela et al. 2012). There, dust temperatures are close to 7 K, and the growth of dust particles due to the forming ice mantles leads to strong gas depletion in the central parts of the cloud (Pagani et al. 2005). In the spectra of the most reddened stars of the background, Whittet et al. (2013)

have detected bands of silicate dust and ices of H_2O , CO, and CO_2 . Their near-infrared polarizations have been measured by Clemens (2012) and Jones et al. (2015).

It was evident that these clouds are relatively close to the Sun because their darkest areas contain very few foreground stars. Different methods have been tried to determine distances to these clouds. Mattila (1979) for LDN 134 applied the method of star counts and polarization of stars projected on the cloud, obtaining a distance of 100 ± 50 pc. For the same cloud, Tomita et al. (1979) applied the increase in extinction A_V with distance for the surrounding stars with photoelectric B, V photometry and MK spectral types, as well as the foreground star counts: the distance to the cloud of ~ 200 pc was accepted. The A_V vs. distance diagram was also used by Snell (1981), who obtained an extinction increase at 160 pc. Franco (1989a,b) applied uvby and H β photometry of 33 Å and F stars in an area covering $8^{\circ} \times 8^{\circ}$ that included vicinities of several clouds in the Ser/Lib complex. A steep increase in extinction at 110 ± 10 pc has been detected, which was accepted as the distance of the complex. Černis & Straižys (1992) published the results of photometry and classification in the Vilnius seven-color system for 14 stars projected on the cloud LDN 134. However, because of the small limiting magnitude, only one reddened star at 140 pc was found to be a useful indicator of the cloud distance. It defines only the largest possible distance to the cloud.

Recently, Green et al. (2014) developed a statistical method for determining distances and reddenings for stars observed in the broad-band five-color system *grizy* of the Pan-STARRS 1

¹ Institute of Theoretical Physics and Astronomy, Vilnius University, Saulėtekio al. 3, Vilnius 10257, Lithuania e-mail: vytautas.straizys@tfai.vu.1t

² Vatican Observatory Research Group, Steward Observatory, Tucson, AZ 85721, USA

³ Jesuit University Ignatianum, Cracow, Poland

⁴ INAF Astronomical Observatory of Padova, 36012 Asiago, VI, Italy

⁵ SOFIA Science Center, USRA, NASA Ames Research Center, Moffett Field, CA 94035, USA

^{*}Full Tables 1 and 2 are only available at the CDS via anonymous ftp to cdsarc.u-strasbg.fr (130.79.128.5) or via http://cdsarc.u-strasbg.fr/viz-bin/qcat?J/A+A/611/A9

survey. Applying this method, Schlafly et al. (2014) estimated distances to dust clouds in the sky area covered by the Pan-STARRS photometry, which also includes the clouds in the Ser/Lib complex. The following distances were obtained: 105 pc for LDN 134, 121 pc for LDN 183, 77 pc for MBM 38, and 88 pc for LDN 1780. Distance uncertainties for LDN 134 and LDN 183 of 7% to 9% are reported.

The present investigation aims to identify more stars in the distance range from 80 to 120 pc of various spectral types (including K and M dwarfs), which could be used for a better estimation of the distance to the Ser/Lib dust cloud complex. For this task, we applied the Vilnius seven-color photometric system, which gives photometric two-dimensional spectral types, extinctions, and distances for stars covering a wide range of spectral classes. This system is in use for the classification of stars in the direction of open clusters, associations, and dark clouds in the presence of variable interstellar reddening (see, e.g., Straižys et al. 2013, 2014a,b, 2015, 2016a,b). Another task is obtaining interstellar extinctions for stars located behind the cloud complex. Combining their extinctions and polarizations will allow investigating dust grain properties in areas of different dust density. With the Gaia DR1 parallaxes, distances to the stars of up to \sim 500 pc are now much more reliable.

2. Photometric data and spectral types

The investigated $2^{\circ} \times 2^{\circ}$ area (Fig. 1) is centered on the cloud LDN 183 at RA (J2000) = $15^{h}54^{m}$, Dec J2000) = $-03^{\circ}00'$. The area also covers the nearby cloud LDN 169. CCD exposures with the filters of the Vilnius seven-color photometric system were obtained with the Maksutov-type 35/51 cm telescope of the Molėtai Observatory in Lithuania. The VersArray 1300B camera (Princeton Instruments) contains a back-illuminated UVenhanced chip with 1340×1300 pixels of $20 \times 20 \mu m$ with liquid nitrogen cooling (Zdanavičius & Zdanavičius 2003; Zdanavičius et al. 2012). The medium-band Vilnius system UPXYZVS with the mean wavelengths at 345, 374, 405, 466, 516, 544, and 656 nm is described in the Straižys (1992) monograph. Since the field of the CCD camera is $1.26^{\circ} \times 1.22^{\circ}$, the whole $2^{\circ} \times 2^{\circ}$ area has been covered by four partly overlapping fields. At the same time, tie-in exposures of the area around the nearby cloud LDN 134 were obtained. As we described above, this area contains 14 stars with magnitudes and colors in the same photometric system measured photoelectrically (Černis & Straižys 1992). These stars were used as zero-point standards for the LDN 183 area. The instrumental magnitudes and colors were transformed to the standard Vilnius system using the linear color equations obtained by observations of the open cluster M 67, where high-precision standards are available (Laugalys et al. 2004). The exposures were processed with the IRAF code in the aperture mode.

The final catalog of magnitudes, color indices, and their uncertainties for 830 stars is given in Table 1. Its limiting magnitude V is close to 15. The uncertainties take into account the signal-to-noise ratios and the errors of the transformation into the standard system. At V=14 mag, the uncertainties for color indices Y-V, Z-V, and V-S are mostly 0.015–0.020 mag; for the violet index X-V. they are 0.020–0.035 mag; for the index P-V, they are 0.035–0.055 mag; and for the index U-V, they are 0.060–0.095 mag. A relatively low accuracy of photometry at the limiting magnitude, especially in the ultraviolet, was related with a large zenith distance of the area and a bright sky background. For stars fainter than $V \approx 14.5$ mag, no two-dimensional spectral types are provided.

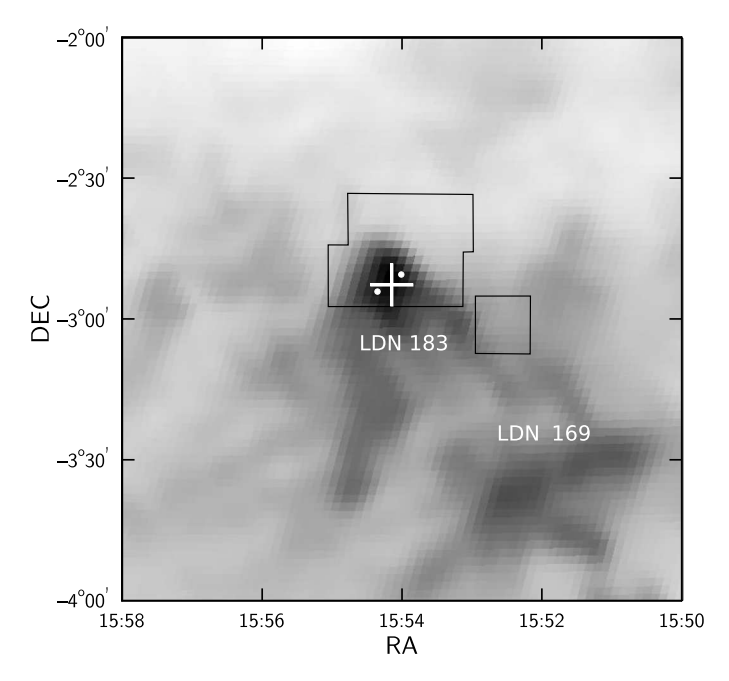


Fig. 1. Areas covered by observations in the Vilnius photometric system. The whole $2^{\circ} \times 2^{\circ}$ area was observed with the Maksutov telescope of the Molètai Observatory, and the seven $12' \times 12'$ areas were observed with the VATT telescope. Six of them form a black irregular rectangle and the seventh is a separate black square. Two heavily reddened red giants, discussed in Sect. 4, are plotted as the white dots. The cross designates the position of the dust peak, according to Pagani et al. (2005). The background is a map of the thermal dust emission at 857 GHz (350 μ m) measured by the *Planck* space mission and taken from the SkyView virtual observatory.

Additionally, seven smaller areas $(12' \times 12')$ in the northern part of LDN 183 were observed in the Vilnius system with the 1.8 m VATT telescope on Mt. Graham, Arizona, using a STA0500A CCD camera with a $4k \times 4k$ chip; the pixel sizes are $15 \times 15 \mu m$, the scale is 0.2"/pixel. The positions of these areas are shown in Fig. 1: six partly overlapping areas form an irregular rectangle, and the seventh is a separate square at 15:52:35, -03:01. These areas were chosen at the edge of the dark cloud to find more stars that are immersed in the front side of the cloud, but not very deeply, to be brighter than the limiting magnitude (V = 20). The VATT areas were tied-in to photoelectric standards in LDN 134 (Černis & Straižys 1992) and the area around the globular cluster M 12 (Zdanavičius et al. 1989). Table 2 contains the catalog of magnitudes, colors, and their uncertainties for 483 stars with V magnitudes between 14 and 20 measured in all seven VATT areas. To avoid confused identifications, we added 1000 to the running numbers of stars in Table 2. The uncertainties of magnitudes and colors down to $V \approx 18$ mag are lower than ±0.03 mag. For most of the fainter stars, except for K and M stars, no two-dimensional spectral types are provided.

For the two-dimensional classification of stars measured in the Vilnius system, two codes were applied. The first is the COMPAR code we described in our previous publications (e.g., Straižys et al. 2013). The method uses matching of 14 different interstellar reddening-free Q-parameters of a program star to those of about 9500 standard stars of various spectral and luminosity classes, metallicities, and peculiarities. The matching of Q-parameters leads to a selection of some standard stars with a set of Qs most similar to those of the program star. The classification accuracy is characterized by the value of σQ , the

mean square difference of Q-parameters of the program star, and the standard star.

The second code used for the classification of stars, called NORMA, has been developed recently by Zdanavičius (in prep.). It uses a set of 808 standards formed from the intrinsic color indices of the Vilnius system for different spectral and luminosity classes from Straižys (1992). First, for each program star, virtual sets of color excesses E_{U-V} , E_{P-V} , E_{X-V} , E_{Y-V} , E_{Z-V} , and E_{V-S} in relation to each of the 808 intrinsic standards are calculated. After rejection of negative values, these six "excesses" for each standard are transformed into E_{Y-V} using color-excess ratios corresponding to the normal interstellar extinction law. After this, the six values of E_{Y-V} with respect to each standard are averaged and their dispersion calculated. The standard, for which all the six values of E_{Y-V} show the minimal dispersion, is accepted as the best analog of the program star. Spectral class, luminosity class, color excess, and absolute magnitude of this standard are ascribed to the considered program star. The classification accuracy is characterized by the value of σE_{Y-V} , the mean square difference of six color excess values. For faint stars of spectral classes K or M, the index U-V, and sometimes P-V, are absent. In these cases, only five or four values of the excesses E_{Y-V} are used to estimate the dispersion. When the dispersion of E_{Y-V} is too high ($\sigma > 0.03$ mag) for all standards, the star is considered to be a binary with components of different spectral classes or a peculiar star.

Both methods have their advantages and limitations. The advantage of the COMPAR method is that it enables identifying stars with various types of peculiarity (metal deficient, Am, Ap, white dwarfs, $H\alpha$ emission stars, etc.). The advantage of the NORMA method is that it considerably better represents stars with different spectral and luminosity classes of the solar chemical composition. The spectral classes and luminosities given by the two methods usually coincide or differ by 1–2 spectral subclasses and one luminosity class. The priority is given to the method that gives a better classification accuracy.

In the investigated area, the normal interstellar extinction law, which for early-type stars gives the standard value of R_{BV} = 3.15, was accepted. In the broad-band BV system (due to the band-width effect) for K-type giants, this standard value corresponds to R_{BV} = 3.5–3.6 (Straižys 1992, Table 11). In the medium-band Vilnius system, the band-width effect is much smaller, but it is taken into account when calculating the ratios of color excesses and Q-parameters. We checked the interstellar extinction law in the area determining the slope of the reddening line of red giants in the J-H vs. H- $K_{\rm S}$ diagram, E_{J} -H/ E_{H} - $K_{\rm S}$. It was found to be close to 1.8–1.9, which corresponds to the normal extinction law (Straižys & Laugalys 2008).

In some cases, the photometric separation of late K- and early M-type stars was problematic. In these cases, we used the two-color diagram $J-K_s$ vs. W1-W2, proposed by Koposov et al. (2015), to identify M dwarfs and M giants. Here J and K_s are 2MASS magnitudes, and W1 and W2 are WISE magnitudes.

The classification accuracy depends on the errors of the observed color indices. If the errors of the colors in the visible part of the spectrum are less than 0.03 mag and in the ultraviolet part are less than 0.04 mag, the accuracy of spectral class is of the order of \sim 2 decimal subclasses. The accuracy of luminosities for B8-A-F-G5 stars of luminosity classes V-IV-III is about one luminosity class. For K-type stars, the classification accuracy is higher – about 0.5 of spectral subclass and 0.5 of luminosity class. K- and M-type stars can be classified even without the ultraviolet U and P magnitudes, thus the errors of color indices

U-V and P-V are not important for the classification of late-type stars

The relation between luminosity classes and absolute magnitudes (see the HIPPARCOS and *Gaia* HR diagrams given by Perryman et al. (1995, 1997) and Gaia Collaboration (2016)) shows that the maximum (or 3σ) error of M_V is about ± 0.5 mag for the majority of A, F, and G stars. The M_V error for K-stars of luminosity classes V, IV–V, and IV is of the same order. However, for K stars of luminosity classes III–IV and III, the accuracy of M_V is lower ($3\sigma \approx 1.0$ mag) because of a steep rise of the sequence of giants in the HR diagram.

Two-dimensional photometric spectral types for about 70% of the observed stars are given in Tables 1 and 2. To designate spectral classes, we use lower-case letters to emphasize that they are obtained from photometric data. The stars with oblong or multiple images within 6" from the central object in the Maksutov exposures and within 1.5" in the VATT exposures were excluded from classification: these stars have the notes "bin" in the spectral type column of Tables 1 and 2. For the stars classified as peculiar and stars with $\sigma_0 > 0.03$, spectral types are not given. In the VATT areas with deep photometry, about 20–30% of the objects are found to be metal-deficient stars. To differentiate metal-deficient dwarfs and giants, the reddeningfree diagrams Q_{UXY} vs. Q_{UYV} and Q_{UPY} vs. Q_{XZS} were used (Bartkevičius & Straižys 1970; Straižys 1992). It seems that the majority of stars that in Tables 1 and 2 are marked as "md:" belong to subdwarfs. Some objects were found to be white dwarfs and galaxies. White dwarfs were identified by the values of the parameter $Q_{UPYV} < 0.0$ (Straižys 1992), and galaxies were identified by the values of the color index J - W1 > 1.7 (Kovács & Szapudi 2015). The published catalogs of faint galaxies (e.g., Kovács & Szapudi 2015; Krakowski et al. 2016) usually avoid the areas with dust clouds.

Tables 1 and 2 contain 14 stars in common. Their V magnitudes coincide within ± 0.05 mag, except for the stars 433 and 434 in Table 1 (1448 and 1451 in Table 2). We suspect that these stars appear brighter in the Maksutov exposures because of the influence of a nearby galaxy. The color indices U-V, P-V, and V-S coincide within ± 0.06 mag and the indices X-V, Y-V, and Z-V within ± 0.04 mag. These differences are in agreement with the expected uncertainties listed in Sect. 2.

To verify the results of photometric classification, 18 stars brighter than V = 12.8 mag were observed spectroscopically with the 1.22 m telescope at the Asiago Observatory and the VATT 1.8 m telescope on Mt. Graham. The Asiago spectra cover the range of wavelengths 3487-5885 Å and have a resolution of 1.17 Å/pixel. The VATT spectra cover the range 3730–6800 Å and have a resolution of 3 Å per two pixels. The VATT spectra were classified visually by comparing them with MK standards of similar resolution. The Asiago spectra were classified by applying the computer program MKCLASS by Gray & Corbally (2014). The results of the classification are given in Table 3, together with the results of our photometric classification. In most cases, the differences between the spectroscopic and photometric spectral types do not exceed 1–2 spectral subclasses and half a luminosity class. Stars 41, 75, and 88 are the close visual binaries WDS J15501-0311AB, J15504-0303AB, and J15505-0215AB, respectively. Their spectral classification can be affected by the secondary components.

The *Gaia* Data Release 1 (Gaia Collaboration 2016) in our $2^{\circ} \times 2^{\circ}$ area lists 79 stars with parallaxes. We have selected 14 stars with d < 200 pc whose distance uncertainties are lower than ± 10 pc.

Table 1. First ten lines of the catalog of 830 stars containing the results of CCD photometry with the Maksutov telescope of the Molètai Observatory and their photometric spectral types.

No.	RA (J2000)		Dec	(J2	000)		V	σV	$U\!\!-\!\!V$	$\sigma(U-V)$	$P\!\!-\!\!V$	$\sigma(P-V)$	$X\!\!-\!\!V$	$\sigma(X\!\!-\!\!V)$	<i>Y</i> – <i>V</i>	$\sigma(Y\!\!-\!\!V)$	Z-V	$\sigma(Z\!\!-\!\!V)$	$V\!\!\!-\!\!\!S$	$\sigma(V-S)$	Photom.
	h	m s		0	′	″		mag	mag	mag	mag	mag	mag	mag	mag	mag	mag	mag	mag	mag	mag	sp. type
1	15:49	:42.6	0 -	-03:	44	:43.3	13.	946	0.014					1.971	0.027	0.816	0.017	0.335	0.019	0.853	0.019	g7 V
2	15:49	:43.4	6 -	-03:	43	:27.7	14.	241	0.015					1.653	0.027	0.746	0.019	0.280	0.021	0.750	0.020	g
															0.017							
									0.012					2.724	0.026	1.061	0.013	0.469	0.015	1.055	0.013	k1 III, bin
5	15:49	:44.7	0 -	-03:	47	13.9	14.	257	0.015	2.914	0.075	2.345	0.052	1.599	0.026	0.688	0.018	0.253	0.021	0.731	0.019	g
									0.015					2.315	0.039	0.939	0.020	0.476	0.022	0.963	0.019	k2 V, bin
7	15:49	:45.6	6 -	-02	47	:11.3	11.	825	0.010	3.238	0.028	2.837	0.021	1.883	0.016	0.759	0.011	0.360	0.011	0.776	0.011	k0.5 V
8	15:49	:45.6	9 -	-03:	46	46.3	14.	236	0.015	3.057	0.081	2.547	0.059	1.710	0.027	0.735	0.018	0.276	0.021	0.682	0.020	g
															0.017							
10	15:49	:46.8	4 -	-02:	44	:00.8	14.	037	0.013	2.878	0.082	2.477	0.052	1.715	0.025	0.767	0.016	0.306	0.018	0.737	0.018	g5:

Notes. The full catalog is available at the CDS.

Table 2. Ten lines of the catalog of 483 stars containing the results of CCD photometry with the VATT telescope and their photometric spectral types.

No.	RA (J2000)	Dec (J2000)	V	σV	$U\!\!-\!\!V$	$\sigma(U\!\!-\!\!V)$	$P\!\!-\!\!V$	$\sigma(P\!\!-\!\!V)$	$X\!\!-\!\!V$	$\sigma(X\!\!-\!\!V)$	$Y\!\!-\!\!V$	$\sigma(Y\!\!-\!\!V)$	$Z\!\!-\!\!V$	$\sigma(Z\!\!-\!\!V)$	$V\!\!-\!\!S$	$\sigma(V - S)$	Photom.
	h m s	o / //	mag	mag	mag	mag	mag	mag	mag	mag	mag	mag	mag	mag	mag	mag	sp. type
1201	15:53:48.15	-02:42:17.9	17.700	0.003	2.866	0.026	2.258	0.021	1.678	0.016	0.735	0.011	0.276	0.012	0.680	0.012	g0 V
1202	15:53:48.43	-02:38:45.0	16.523	0.001	2.675	0.021	2.162	0.018	1.574	0.015	0.698	0.010	0.280	0.010	0.632	0.010	g0 V
		-02:44:49.5															
1204	15:53:48.98	-02:38:02.0	17.957	0.005	3.117	0.034	2.720	0.032	1.950	0.017	0.796	0.013	0.359	0.013	0.757	0.013	k1 V
1205	15:53:49.12	-02:43:43.5	17.373	0.004	3.134	0.022	2.639	0.019	1.814	0.017	0.759	0.012	0.315	0.012	0.749	0.012	g8 V
1206	15:53:49.29	-02:36:20.1	17.702	0.003	2.672	0.024	2.184	0.022	1.612	0.016	0.710	0.011	0.282	0.011	0.656	0.012	g, md:
		-02:38:54.8															
1208	15:53:49.34	-02:37:09.6	15.683	0.011	3.203	0.020	2.746	0.018	1.917	0.015	0.778	0.010	0.327	0.010	0.737	0.010	g9.5 V
		-02:46:50.2													0.815		
1210	15:53:49.40	-02:42:56.5	16.207	0.002			2.964	0.019									k0.5 V

Notes. The full catalog is available at the CDS.

3. Interstellar extinctions and distances

For 534 stars from Table 1 and for 248 stars from Table 2 with spectral and luminosity classes, we calculated the color excess E_{Y-V} , interstellar extinction A_V , and distance d (in pc) with the following equations:

$$E_{Y-V} = (Y-V)_{\text{obs}} - (Y-V)_0,$$
 (1)

$$A_V = 4.16 \, E_{Y-V},\tag{2}$$

$$\log d = 0.2 (V - M_V + 5 - A_V), \tag{3}$$

where V and Y-V are the observed magnitudes and color indices. The intrinsic color indices $(Y-V)_0$ and absolute magnitudes M_V for a given spectral type are adopted from Straižys (1992). The coefficient 4.16 in Eq. (2) corresponds to the normal extinction law. The distance errors are between -0.93~d and +1.08~d for B8-A-F-G5 V-III stars and G8-K dwarfs, and between -0.86~d and +1.16~d for G8-K5 stars of luminosities III and III-IV. The typical extinction error A_V is $\sigma \approx \pm 0.10$ mag. This error mostly depends on the uncertainty of the spectral classes, while the error of the luminosity class is less important. For stars close to the limiting magnitude, the accuracy of the observed magnitudes and colors decreases, and this leads to uncertain classification, extinctions, and distances.

4. Discussion

The plot of the extinction A_V vs. distance for 57 stars up to 200 pc, classified in the Vilnius system, is shown in Fig. 2. Since most stars are brighter than V = 14 mag, their classification, extinctions, and distances are reliable. Stars with photometric distances are plotted as dots, and those with distances calculated from Gaia parallaxes are plotted as open circles with the error crosses. The error crosses are also shown for four stars with photometric distances, lying on the rising part of the extinction. To avoid overcrowding, the error crosses for other stars with photometric distances are not shown. Instead, the error bars of distance (in red) for photometric distances at 100 and 180 pc are shown at the top of the figure. The photometric distance errors of dots at 100 pc are about $\pm 8-10$ pc, that is, they are comparable to the Gaia DR1 distance errors. The broken curve in Fig. 2 shows the expected run of the extinction with distance in the Galactic diffuse dust layer calculated with the exponential Parenago (1945) equation for the Galactic latitude of LDN 183 ($b = 36.75^{\circ}$) and the extinction coefficient $a_0 = 1.25 \text{ mag kpc}^{-1}$.

Figure 2 shows that between the distances 100 and 130 pc, a steep increase of the extinction takes place. The mean distance to the three reddened K dwarfs 100, 424, and 753, nearest to the Sun, is 104.7 pc. This distance is within their error bars. Thus, we will accept that the front edge of the cloud is at 105 ± 8 pc distance.

Table 3. Stars with spectral types based on the VATT and Asiago spectra.

No.	V	Sp (VATT)	Sp (Asiago)	Sp (photom.)	Sp (other)
39	10.498	K0 V	K1 V	k0 V	_
41	9.467	F5 V	F6 IV-V	f2 V	F2 [1]
45	9.948	K3 V	K2 V	k2 V	K2 [2]
75	8.506	F3 III	F2 IV	f2 V	F2 V [3]
86	10.370	K4.5 V	K5 V	k4 V	K5 [4]
88	9.457	F5 V	F5 IV-V	f4 V	F3/5 V [3]
167	12.375	K4 V	_	k3 V	_
221	12.652	K7 V	_	k7 V	K: [5]
229	8.516	F9 V	F8 V	f9 V	G0 (HD), G1 V [3]
298	11.425	K2+ V	_	k2.5 V	_
301	9.257	F7 V	F7 IV-V	f5 V	F7 V [3]
392	10.866	F9 IV	F7 IV-V	g2 IV	_
452	10.195	F8 V	F9 V	f8 V	_
611	10.008	K3 III	K0 IV CN	k3 III	_
626	11.395	G1 V	G0 IV-V	g2 V	_
753	11.561	K3.5 V	K5 V	k3 V	_
763	12.855	K7 V	_	k7 V	_
777	12.356	M1 V	M0 V	m2 V	M2 [6]

Notes. Star numbers are taken from Table 1. For the comparison, photometric spectral types are given. The last column lists the spectral types from the literature. Stars 41, 75, and 88 are visual binaries (see the text).

References. [1] Upgren & Staron (1969); [2] Heckmann (1975); [3] Houk & Swift (1999); [4] Stephenson (1986); [5] Giclas et al. (1959); [6] Lepine & Gaidos (2011).

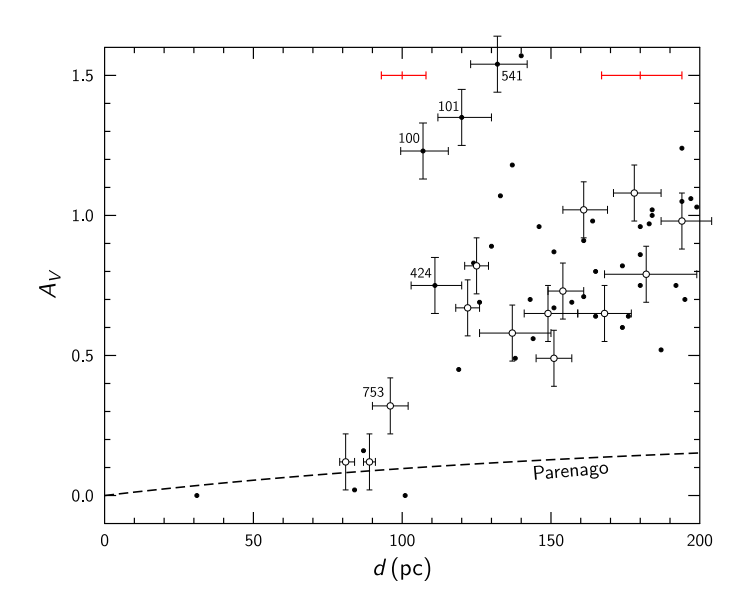


Fig. 2. Dependence of the extinction on distance for the investigated area up to d=200 pc. Stars with photometric distances are plotted as dots and stars with *Gaia* distances as circles. The stars with *Gaia* distances and four numbered stars with photometric distances on the rising part of the extinction are shown with the error crosses. The black broken curve designates the extinction rise with distance in the diffuse Galactic dust layer for $b=+36.75^{\circ}$ according to the exponential Parenago (1945) law.

Figure 2 shows a tendency for the increase in extinction between 100 and 130 pc to be slightly slanted. The run of the extinction can be approximated by a line starting from the Parenago curve at d = 105 pc and ending at star 541 (d = 132 pc, $A_V = 1.54$). This would mean that the dust layer has a depth of about 20 pc. This depth value is in agreement with the observable size of the Ser/Lib cloud complex, which covers not less than

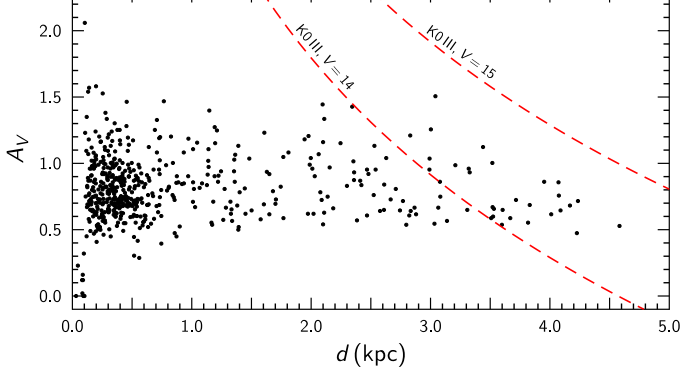


Fig. 3. Dependence of the extinction on distance for the investigated area up to d = 5 kpc based on 534 stars observed with the Maksutov telescope down to V = 15 mag. The red broken curves show the effect of limiting magnitudes for K0 III stars of magnitudes 14 and 15.

 $10^{\circ} \times 10^{\circ}$. However, the central dense core of LDN 183 with a diameter of about 15' has a subparsec size.

Figures 3 and 4 show the extinction vs. distance plots for the Maksutov and VATT stars up to d=5 kpc. They both indicate that behind the cloud, located close to 110 pc, the extinction remains more or less at the same level, covering the values of A_V between 0.5 mag and 2.0–2.5 mag. The stars with higher extinctions are not observed due to limiting magnitude effects, shown by the limiting magnitude curves for K0 giants of magnitudes V=14 and 15 in Fig. 3 and for G0, G5, and K0 main-sequence stars of magnitudes V=19 in Fig. 4. These types of stars are most frequent among the distant stars in Figs. 3 and 4, respectively. The maximum values of the extinction in Figs. 3 and 4 represent only the outer edges of the dense clouds LDN 183 and LDN 169, and the space around them.

The LDN 183 cloud in its central part is so dense that medium-band photometry in the blue and ultraviolet up to

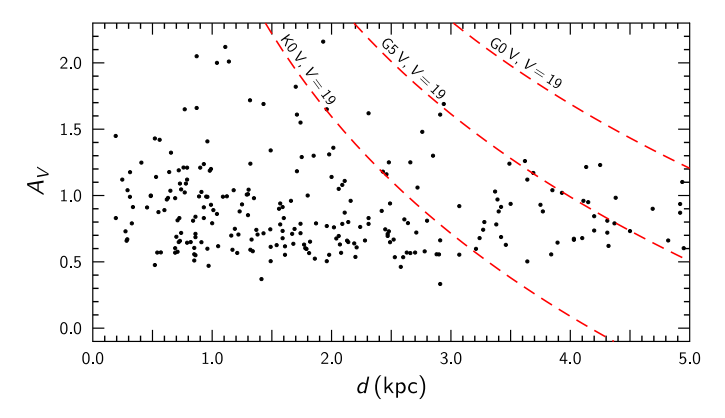


Fig. 4. Dependence of the extinction on distance for the investigated area up to d = 5 kpc based on 248 stars observed with the VATT telescope with the magnitudes V from 12 to 20. The red broken curves show the effect of limiting magnitudes for G0 V, G5 V, and K0 V stars of V = 19 mag.

V=20 mag does not allow observing and classifying stars that are located behind the cloud. Whittet et al. (2013) from infrared spectra, obtained with the IRTF telescope at Mauna Kea and the *Spitzer* Space Telescope, determined spectral types for nine background G-K-M giants selected from the J-H vs. $H-K_s$ diagram that are located close to the center of LDN 183. Two of these stars, AllWISE J155400.28-025032.3 (G8 III, $K_s=10.786$) and J155420.44-025407.5 (K3 III, $K_s=7.910$), exhibit A_V values between 13 and 14 mag. In Fig. 1 these two stars are plotted as white dots. Pagani et al. (2004), applying photometry in the H and K passbands down to 21 mag, obtained A_V up to \sim 30 mag. Even higher values of the extinction are estimated by Pagani et al. (2003, 2004) from the absorption in the ISOCAM 7 μ m maps. Juvela et al. (2002) reported an extinction value of $A_V \approx 17$ mag, which they estimated from the emission of dust at 200 μ m.

5. Conclusions

We presented photometry in the Vilnius seven-color system for 1299 stars located within the $2^{\circ} \times 2^{\circ}$ area in the direction of the high-latitude clouds LDN 183 and LDN 169. For 782 stars we determined spectral and luminosity classes, color excess, interstellar extinction A_V , and distance. The results were applied to investigate interstellar extinction in the area and to determine the cloud distance by combining photometric extinctions and distances with the *Gaia* trigonometric parallaxes.

The investigation shows that the distance to the front edge of the clouds LDN 183 and LDN 169 is close to 105 ± 8 pc. This result is based on photometric extinctions and distances as well as on the *Gaia* parallaxes. This distance is in a good agreement with the results obtained by Franco (1989a) from Strömgren photometry and by Green et al. (2014) from the Pan-STARRS 1 survey. It is also possible (see Fig. 2) that the dust layer in the direction of the Ser/Lib cloud complex has a thickness of about 20 pc, in agreement with its surface extent. The extinction A_V across this layer in the outer parts of the clouds and between the clouds is on the order of 0.5–2.0 mag.

Acknowledgments. This research has made use of the SIMBAD database, operated at the CDS, Strasbourg, France, the SkyView Virtual Observatory of NASA, and the NASA/IPAC Extragalactic Database (NED) operated by the JPL at California Institute of Technology. We have also used the data from DR1 of the European Space Agency (ESA) mission *Gaia*, and the products from the 2MASS project of the University of Massachusetts and the Infrared Processing and Analysis Center/California Institute of Technology, funded by the NASA and NSF, and from the NeoWISE project of the JPL of California Institute of Technology, funded by the Planetary Science Division of NASA. Preliminary results of this investigation were presented at the AAS Meeting No. 229 (Boyle et al. 2017). We are grateful to Vygandas Laugalys for his help in observations and reductions.

References

```
Bartkevičius, A., & Straižys, V. 1970, Bull. Vilnius Obs., 30, 16
Boyle, R. P., Janusz, R., Straižys, V., et al. 2017, AAS Meeting, 229, 142.10
Černis, K., & Straižys, V. 1992, Baltic Astron., 1, 163
Clemens, D. P. 2012, ApJ, 748, 18
Franco, G. A. P. 1989a, A&A, 223, 313
Franco, G. A. P. 1989b, A&AS, 80, 127
Gaia Collaboration (Brown, A. G. A., et al.) 2016, A&A, 595, A2
Giclas, A. L., Slaughter, C. D., & Burnham, R. 1959, Lowell Obs. Bull., 4, 136
Gray, R. O., & Corbally, C. J. 2014, AJ, 147, 80
Green, G. M., Schlafly, E. F., Finkbeiner, D. P., et al. 2014, ApJ, 783, 114
Heckmann, O. 1975, AGK3 Star Catalogue of Positions and Proper Motions
   North of -2.5 deg Declination (Hamburg-Bergedorf: Hamburger Sternwarte)
Houk, N., & Swift, C. 1999, Michigan Catalogue of Two-Dimensional Spectral
   Types for the HD Stars (Ann Arbor, MI: University of Michigan), 5
Jones, T. J., Bagley, M., Krejny, M., et al. 2015, AJ, 149, 31
Juvela, M., Mattila, K., Lehtinen, K., et al. 2002, A&A, 382, 583
Juvela, M., Ristorcelli, I., Pagani, L., et al. 2012, A&A, 541, A12
Koposov, S. E., Belokurov, V., Zucker, D. B., et al. 2015, MNRAS, 446, 3110
Kovács, A., & Szapudi, I. 2015, MNRAS, 448, 1305
Krakowski, T., Malek, K., Bilicki, M., et al. 2016, A&A, 596, A39
Lallement, R., Welsh, B. Y., Vergely, J. L., et al. 2003, A&A, 411, 447
Laugalys, V., Kazlauskas, A., Boyle, R. P., et al. 2004, Baltic Astron., 13, 1
Lepine, S., & Gaidos, E. 2011, AJ, 142, 138
Lynds, B. T. 1962, ApJS, 7, 1
Magnani, L., Blitz, L., & Mundy, L. 1985, ApJ, 295, 402
Mattila, K. 1979, A&A, 78, 253
Pagani, L., Lagache, G., Bacmann, A., et al. 2003, A&A, 406, L59
Pagani, L., Bacmann, A., Motte, F., et al. 2004, A&A, 417, 605
Pagani, L., Pardo, J.-R., Apponi, A. J., et al. 2005, A&A, 429, 181
Parenago, P. P. 1945, AZh, 22, 129
Perryman, M. A. C., Lindegren, L., Kovalevsky, J., et al. 1995, A&A, 304, 69
Perryman, M. A. C., Lindegren, L., Kovalevsky, J., et al. 1997, A&A, 323, L49
Schlafly, E. F., Green, G., Finkbeiner, D. P., et al. 2014, ApJ, 786, 29
Snell, R. L. 1981, ApJS, 45, 121
Steinacker, J., Pagani, L., Bacmann, A., & Guieu, S. 2010, A&A, 511, A9
Stephenson, C. B. 1986, AJ, 91, 144
Straižys, V. 1992, Multicolor Stellar Photometry (Tucson, AZ: Pachart Publish-
   ing House), available at
   http://www.itpa.lt/MulticolorStellarPhotometry/
Straižys, V., & Laugalys, V. 2008, Baltic Astron., 17, 253
Straižys, V., Boyle, R. P., Janusz, R., et al. 2013, A&A, 554, A3
Straižys, V., Maskoliūnas, M., Boyle, R. P., et al. 2014a, MNRAS, 438, 1848
Straižys, V., Milašius, K., Boyle, R. P., et al. 2014b, AJ, 148, 89
Straižys, V., Vrba, F. J., Boyle, R. P., et al. 2015, AJ, 149, 161
Straižys, V., Čepas, V., Boyle, R. P., et al. 2016a, A&A, 585, A31
Straižys, V., Čepas, V., Boyle, R. P., et al. 2016b, A&A, 590, A21
Tomita, Y., Saito, T., & Ohtani, H. 1979, PASJ, 31, 407
Upgren, A. R., & Staron, R. T. 1969, ApJ, 157, 327
Whittet, D. C. B., Poteet, C. A., Chiar, J. E., et al. 2013, ApJ, 774, 102
Zdanavičius, J., & Zdanavičius, K. 2003, Baltic Astron., 12, 642
Zdanavičius, K., Meištas, E., & Vansevičius, V. 1989, Bull. Vilnius Obs., 84, 3
Zdanavičius, K., Straižys, V., Zdanavičius, J., et al. 2012, A&A, 544, A49
```